Water-level oscillations caused by volumetric and deviatoric dynamic strains

Eyal Shalev,[1] Ittai Kurzon,[1] Mai-Linh Doan[2] and Vladimir Lyakhovsky[1]

[1] *Geological Survey of Israel,* 30 *Malkhe Israel, Jerusalem,* 95501 *Israel.* E-mail: *eyal@gsi.gov.il*

[2] *Institut des Sciences de la Terre (ISTerre), Université Grenoble-Alpes, Grenoble, France*

SUMMARY

Travelling seismic waves and Earth tides are known to cause oscillations in well water levels due to the volumetric strain characteristics of the ground motion. Although the response of well water levels to *S* and Love waves has been reported, it has not yet been quantified. In this paper we describe and explain the behaviour of a closed artesian water well (Gomè 1) in response to teleseismic earthquakes. This well is located within a major fault zone and screened at a highly damaged (cracked) sandstone layer. We adopt the original Skempton approach where both volumetric and deviatoric stresses (and strains) affect pore pressure. Skempton's coefficients *B* and *A* couple the volumetric and deviatoric stresses respectively with pore pressure and BK_u and *N* are the equivalent coupling terms to volumetric and deviatoric strains. The water level in this well responds dramatically to volumetric strain (*P* and Rayleigh waves) as well as to deviatoric strain (*S* and Love waves). This response is explained by the nonlinear elastic behaviour of the highly damaged rocks. The water level response to deviatoric strain depends on the damage in the rock; deviatoric strain loading on damaged rock results in high water level amplitudes, and no response in undamaged rock. We find high values of $N = 8.5$ GPa that corresponds to $-0.5 < A < -0.25$ expected at highly damaged rocks. We propose that the Gomè 1 well is located within fractured rocks, and therefore, dilatancy is high, and the response of water pressure to deviatoric deformation is high. This analysis is supported by the agreement between the estimated compressibility of the aquifer, independently calculated from Earth tides, seismic response of the water pressure and other published data.

Key words: Geomechanics; Permeability and porosity; Wave propagation; Rheology and friction of fault zones.

1 INTRODUCTION

Pore pressure oscillations have been shown to correlate with dynamic volumetric strain changes associated with tides and passage of seismic waves (e.g. Cooper *et al.* 1965; Liu *et al.* 1989; Roeloffs 1996; Ohno *et al.* 1997; Brodsky *et al.* 2003; Kano & Yanagidani 2006; Kitagawa *et al.* 2011). It is commonly assumed that water level in the far field responds only to *P* and Rayleigh waves that are alternately compressional and extensional (Kano & Yanagidani 2006). Water level responses to *S* waves were assumed to be related to the mode conversion of the shear wave to a compressional wave (*SV*) at the free surface (Kano & Yanagidani 2006) or to anisotropic poroelastic response (Brodsky *et al.* 2003). Sterling & Smets (1971), Brodsky *et al.* (2003) and Wang *et al.* (2009) showed that water-level also oscillates in response to Love waves and attributed this to anisotropic poroelastic response as well. However, no quantification has been provided to *S* and Love phases' hydroseismograms.

The role of the shear stress on pore pressure in quasi static loading was demonstrated in the laboratory (Skempton 1954; Lockner

& Stanchits 2002) and by numerical analysis of Coulomb stress maps (Wang 1997). Although in standard poroelasticity (Biot 1941; Wang 2000), changes in deviatoric stress do not induce pore pressure changes, Wang (1997) and Lockner & Stanchits (2002) demonstrated that the deviatoric stress significantly affects the pore pressure. Hamiel *et al.* (2005) showed that nonlinear elastic response of highly cracked or damaged rocks predicts a strong coupling between the deviatoric stresses and the pore pressure.

The goal of this paper is to show and quantify the role of *P*, *S*, Love and Rayleigh waves in inducing pore pressure oscillations and to compare the results with tidal analysis.

2 GOMÈ 1 WELL

The artesian Gomè 1 well is located 80 m from a major fault that defines the western boundary of the Hula pull-apart along the Dead Sea Transform (DST), 33°9′4″N Lat, 35°34′10.4″E Long (Fig. 1). The 396 m deep well was drilled down to the Kurnub sandstone
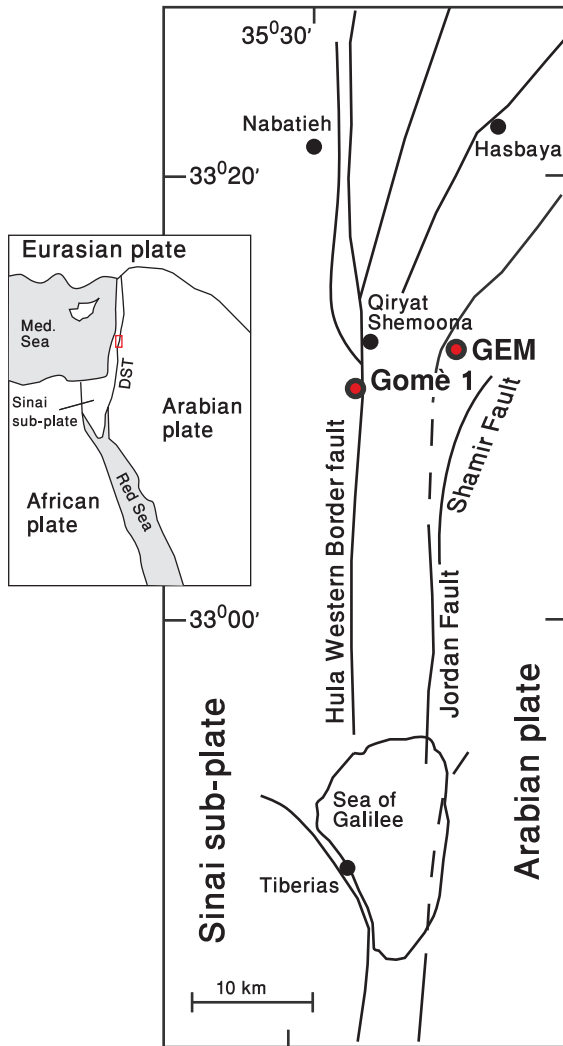
Figure 1. Map of the main fault segments of the Dead Sea Transform (DST) in northern Israel and southern Lebanon (after Sneh & Weinberger 2003). Groundwater pressure data are measured in Gomè 1 well and seismological data are measured in Givat Ha'em (GEM).

group that is confined by a 70 m thick clay layer. Gomè 1 is an artesian (closed) well with water pressure of ~0.08 MPa. The deepest 100 m of the well are installed with screens against the highly permeable layers (~60 m) and casing against the clay layers (~40 m). Water pressure is monitored since 2012 June 6 using Keller–Druck 33 PA transmitter with a set range of 0–0.1 MPa. The accuracy and precision of this transmitter are 50 and 2 Pa, respectively. Temperature dependencies and nonlinearities of the sensor are compensated by the sensor. The analogue output signal of the transmitter in the range of 0–5 V is read by the Analog to Digital (A/D) convertor and saved in the internal memory of the Campbell Scientific CR800 data logger. Water pressure is recorded at 10 sps. In addition, barometric pressure is monitored using Vaisala PTB110. Once a day, data is damped into an external memory device Campbell Scientific SC115 2 GB flash memory drive. The system is powered by a 12 V battery which is recharged by a solar panel. Both seismic response to distant earthquakes and tidal analysis were done using this record.

Only short duration pumping tests (<180 min) were performed in Gomè 1 well. In these pumping tests the well was opened, allowing free discharge from the artesian well. The discharge from

the well was ~0.075 m³ min⁻¹ resulting with a total pumped volume of 13.5 m³. Given the 16.4 m³ volume of the well the results are not reliable and represent the upper limit of the transmissivity. Transmissivity of $T = 4 \times 10^{-4}$ m² s⁻¹ was determined from these pumping tests. As will be shown later, the transmissivity calculated from earth tides is smaller than the one determined from pumping tests.

3 SEISMIC DATA

Seismic data were obtained from the Geophysical Institute of Israel network station Givat Ha'em (GEM), 11 km North-east of Gomè 1 well. GEM is a broad-band seismic station, with a third-generation STS-2 sensor (Streckeisen), and a Europe Trident digitizer (Nanometrics), set to a 40 V peak to peak sensitivity, and to a sample rate of 40 samples per second. Four distant earthquakes were recorded at Gomè 1 well and GEM: 2013 May 24 $M_w = 8.3$ Sea of Okhotsk (epicentral distance $\Delta = 77.011°$); 2013 September 24 $M_w = 7.7$ Pakistan ($\Delta = 26.469°$); 2013 October 12 $M_w = 6.4$ Crete, Greece ($\Delta = 10.396°$); and 2014 May 24 $M_w = 6.9$ Aegean Sea ($\Delta = 10.822°$). Water pressure measured in Gomè 1 correlates with ground velocity for both pressure waves (Fig. 2a) and shear waves (Fig. 2b). The remarkable coupling between ground deformation and water pressure in the shear wave phase (slope = 9.3×10^5 Pa (m s⁻¹)⁻¹) is the same order of magnitude as in the pressure wave phase (slope = 2×10^6 Pa (m s⁻¹)⁻¹). To the best of our knowledge, this linear relation was not studied, and the goal of this paper is to quantify this coupling. We choose to demonstrate this coupling mainly on surface waves because (1) the water pressure and ground velocity amplitudes are relatively low for *P* and *S* body waves, and (2) surface waves are more consistent and reliable in their incidence angle (0⁰) than body waves, affecting the validity of the resulting strain tensor calculation. While on the one hand, the relatively close earthquakes (Crete and Aegean Sea) do not show a good separation between Love and Rayleigh phases, and on the other hand, for the relatively distant earthquakes (Sea of Okhotsk) the amplitudes are very small, the intermediate distant earthquake (Pakistan) has the best waveform that shows this coupling (Fig. 3). The surface waves' path, originating in Pakistan and moving west through the continental complex crust of the Zagros mountains, and possibly other complexities on its continental path to northern Israel, leaves a signature seen as significant anomalies of the particle motion for both the Love and Rayleigh phases. Both waves are seen on all three components, but still the Love waves have larger transversal component than radial and vertical components and are less dispersive, while the Rayleigh waves have larger radial and vertical components than transversal component and show stronger dispersion than the Love packet. Similar observations were observed and reported especially for surface waves propagating through crustal central Asia (Patton 1980; Keilis-Borok 1989; Levshin *et al.* 1992). The emphasis in our analysis is the difference between the volumetric and deviatoric strain effects of seismic waves on pore pressure. Therefore, although in our data, Love waves have large radial and vertical components and Rayleigh waves have large transversal component, the effect of volumetric and deviatoric strains could still be separated as described below. During the passage of the waves, there is an average water pressure decline that is shown as 'sustained change' (Fig. 3d). Similar sustained water level changes have been reported by several authors (Roeloffs 1998; Brodsky *et al.* 2003; Yan *et al.* 2014; Shi *et al.* 2015) and are beyond the scope of this paper which focuses on the water pressure oscillations.
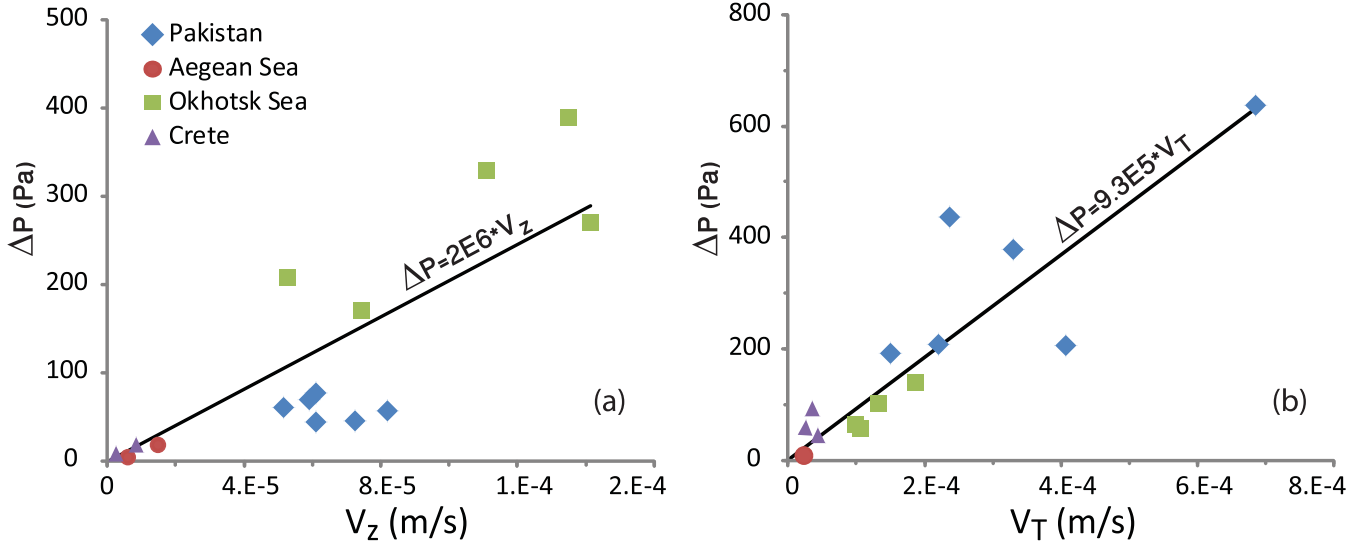
Figure 2. Ground velocity recorded in GEM versus pore pressure as recorded in Gomè 1 well for four different distant earthquakes during (a) *P* wave phase and (b) *S* wave phase.

4 COUPLING STRAIN AND PORE PRESSURE

The amplitude of water-level oscillations in a well in response to seismic waves depends on the characteristics of seismic waves, aquifer properties and geometrical dimensions of the well (Cooper *et al.* 1965). Kitagawa *et al.* (2011) developed an expression describing the hydraulic coupling between the aquifer and the well. According to their results, for parameters of Gomè 1 well aquifer properties and geometrical dimensions of the well have negligible effect on water pressure amplitudes in response to surface waves (see Appendix B). We therefore consider only the poroelastic response of the aquifer to seismic waves and ignore the negligible amplification of the water pressure due to aquifer properties and well geometry.

Skempton (1954) allowed for the possibility that deviatoric stress changes might also affect pore pressure

$$\Delta p_f = -B \left[\Delta\sigma_m + 2\left(A - \frac{1}{3}\right)\Delta\sigma_d \right], \quad (1)$$

where A and B are the Skempton coefficients, $\sigma_m = \frac{1}{3}(\sigma_1 + \sigma_2 + \sigma_3)$ is the mean stress and $\sigma_d = \frac{\sigma_1 - \sigma_3}{2}$ is the deviatoric stress for uniaxial loading ($\sigma_2 = \sigma_3$). Henkel & Wade (1966) and Holtz & Kovacs (1981) generalized (1) to a three-dimensional state of stress but the case of arrival of seismic wave front is simplified to a two-dimensional problem.

Because seismic data is collected by recording ground velocity, we write eq. (1) in terms of strain:

$$\Delta p_f = BK_u \varepsilon_v + N\varepsilon_d, \quad (2)$$

where K_u is the undrained bulk modulus (Wang 2000), ε_v is the volumetric strain, $N = -4\mu B(A - \frac{1}{3})$ is the shear strain coupling coefficient, μ is the shear modulus and $\varepsilon_d = \frac{\varepsilon_1 - \varepsilon_3}{2}$ is the deviatoric strain.

For a linear poroelastic material with no volumetric-shear coupling, $A = 1/3$, $N = 0$. Rocks under shear loading develop fractures and dilate. This nonlinear behaviour could be addressed with damage rheology with an additional modulus (γ) of a damaged solid which couples the volumetric and shear deformation components

(e.g. Lyakhovsky *et al.* 1997). N and A could be expressed as (see Appendix A):

$$N = \frac{8BK_u\gamma(2\mu + \gamma)}{4(2\mu + \gamma)\gamma - 3(6\mu + \gamma)(K_u + 4/3\gamma)} \quad (3)$$

$$A = \frac{1}{3} - \frac{4K_u\gamma}{4(2\mu + \gamma)\gamma - 3(6\mu + \gamma)(K_u + 4/3\gamma)}. \quad (4)$$

The properties B, K_u, μ, γ evolve with a scalar damage parameter α_D, which is a measure of crack concentration $BK_u =$ const; $\mu = \mu_{0+}\alpha_D\xi_0$ γ; $\gamma = \alpha_D\gamma_r$. $\alpha_D = 0$ corresponds to intact rock and $\alpha_D = 1$ for completely destroyed rock. As damage accumulates, the coupling between volumetric and shear strain increases.

The relation between fluid pressure and strain components are estimated here using tidal and seismic analysis. With this relation, we can finally estimate the damage of the rock in the study area. Because the deformations associated with tides and distant seismic waves are infinitesimal smaller than tectonic and lithostatic strains, we can use linear stress-strain relations with damage dependent effective properties.

4.1 Tidal analysis

The analysis of the volumetric strain changes due to tidal forcing assumes that the horizontal strains are determined by the elastic properties of the earth as a whole (Bredehoeft 1967). The poroelastic property determined from the tidal phase shift and amplitude results is (Doan *et al.* 2006):

$$BK_u \frac{1 - 2\nu_u}{1 - \nu_u} = p_f \frac{ga}{W} \frac{1}{(2h - 6l)}, \quad (5)$$

where B is the volumetric Skempton coefficient, K_u is the undrained bulk modulus, ν_u is the undrained Poisson ratio, p_f is the well-head water pressure, $g = 9.81$ m s^{-2} is local gravity acceleration, $a = 6371023.6$ m is Earth radius, W is tidal potential, $h = 0.606$ is Love coefficient and $l = 0.084$ is Shida coefficient. Following Hsieh *et al.* (1987), the phase shift and amplitude of the cross-correlation
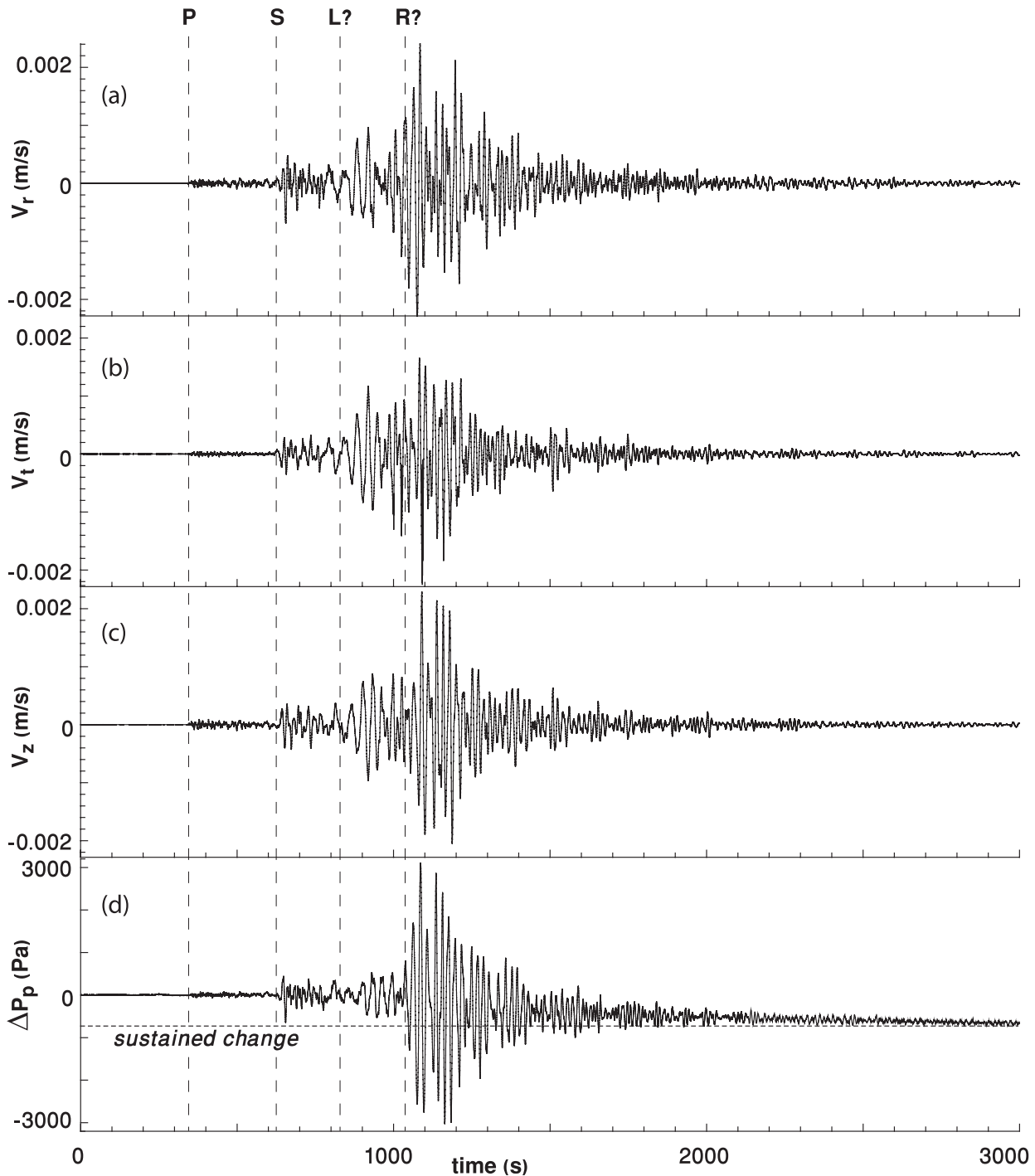
Figure 3. $M_w = 7.7$, 2013 September 24 Pakistan earthquake Seismogram and water well response. (a) Radial, (b) transversal and (c) vertical component of seismogram recorded at GEM, and (d) water level changes recorded at Gomè 1 well. The arrivals of Pressure (P), Shear (S), Love (L) and Rayleigh (R) waves are marked with dashed lines. The arrivals of Love and Rayleigh waves are questionable because they both have radial, transversal and vertical components. However, the separation between these two phases is not done and not important in our analysis.

between water pressure and earth tides is also used to determine the transmissivity (Appendix B).

4.2 Strain in seismic waves

4.2.1 Surface waves

Love and Rayleigh waves traveling along earth's surface far enough from the source (plain waves) are assumed to have displacements

varying in the direction of wave propagation (R) and decaying with depth (Z); hence, the transversal strain $\varepsilon_{TT} = 0$. Because we are close to free surface

$$\sigma_{ZZ} = \lambda^e \varepsilon_v + 2\mu^e \varepsilon_{ZZ} + B K_u \alpha_B \varepsilon_v = 0 \tag{6a}$$

$$\sigma_{RZ} = 2\mu^e \varepsilon_{RZ} = 0 \tag{6b}$$

$$\sigma_{TZ} = 2\mu^e \varepsilon_{TZ} = 0 \tag{6c}$$

where $\varepsilon_v = (\varepsilon_{RR} + \varepsilon_{TT} + \varepsilon_{ZZ})$, λ^e and μ^e (shear) are the effective Lamé moduli, and α_B is Biot coefficient. Solving (6a) for ε_{zz}, using $\varepsilon_{TT} = 0$, gives

$$\varepsilon_{ZZ} = -\frac{\lambda^e + BK_u\alpha_B}{\lambda^e + 2\mu + BK_u\alpha_B}\varepsilon_{RR} \tag{7}$$

and the volumetric strain

$$\varepsilon_v = \varepsilon_{RR} + \varepsilon_{ZZ} = \left(1 - \frac{\lambda^e + BK_u\alpha_B}{\lambda^e + 2\mu^e + BK_u\alpha_B}\right)\varepsilon_{RR} = \frac{1-2\nu_u}{1-\nu_u}\varepsilon_{RR}. \tag{8}$$

The strain perturbation caused by the seismic waves can be calculated from the seismic velocities:

$$\varepsilon_{RR} = \frac{\partial u_R}{\partial R} = \frac{v_R}{V_{R,L}} \tag{9a}$$

$$\varepsilon_{RT} = \frac{1}{2}\frac{\partial u_T}{\partial R} = \frac{1}{2}\frac{v_T}{V_{R,L}}, \tag{9b}$$

where u_R and v_R are the radial ground motion (displacement and velocity), u_T and v_T are the transversal components, $V_{R,L}$ is the either Rayleigh (3.5 km s^{-1}) or Love (3 km s^{-1}) wave velocity depending on the considered phase (e.g. Lay & Wallace 1995). Substituting eq. (6a) into eq. (5) gives

$$\varepsilon_v = \frac{1-2\nu_u}{1-\nu_u}\frac{v_R}{V_{R,L}}. \tag{10}$$

Substituting ε_v (eq. 10) and $\varepsilon_d = \varepsilon_{RT}$ (eq. 9b) into eq. (2) gives the calculated pore pressure

$$\Delta p_f = BK_u\frac{1-2\nu_u}{1-\nu_u}\frac{v_R}{V_{R,L}} + N\frac{1}{2}\frac{v_T}{V_{R,L}} \tag{11}$$

which is correlated to the measured pore pressure in the well, associated with Love and Rayleigh waves. The same term ($BK_u\frac{1-2\nu_u}{1-\nu_u}$) can be independently calculated by tidal analysis (eq. 5) and by hydro-seismic data processing (eq. 11).

4.2.2 Body waves

For the location of the Pakistan event ($\Delta = 26.469°$) the incident angle is almost vertical and the volumetric strain is estimated as

$$\varepsilon_v = \frac{\partial u_Z}{\partial Z} = \frac{v_Z}{V_{P,S}} \tag{12}$$

and the deviatoric strain is estimated as

$$\varepsilon_d = \frac{1}{2}\frac{\partial u_T}{\partial Z} = \frac{1}{2}\frac{v_T}{V_{P,S}}, \tag{13}$$

where $V_{P,S}$ is either the *P*-wave velocity of the *S*-wave velocity (2500 and 1500 m s^{-1} respectively) depending on the considered phase. Both phases are showing free-surface-reflection amplification term (e.g. Shearer 2009), hence the strains are divided by two. Substituting ε_v (eq. 12) and ε_d (eq. 13) into eq. (2) gives the calculated pore pressure, which is fitted to the measured pore pressure in the well associated with *P* and *S* waves.

While for the Love and Rayleigh surface waves, the basic assumption for strain calculation is rigorous, for *P* and *S* waves, the estimated strain components are not well resolved due to the following uncertainties: (1) the incidence angle is not necessarily vertical; (2) there are multiple phases within the same wave-packets; (3) the amplitude of these phases are low relatively to the ambient noise.

5 DATA PROCESSING

The three velocity channels (ENZ) and the fluid pressure were segmented and aligned by the origin time of the event. The three velocity channels were rotated horizontally to the Radial and Transversal components, and then picked for their P, S, Love and Rayleigh arrivals. Calculated strains (eqs 10–13) and measured fluid pressure were demeaned and smoothed using high-pass ButterWorth filter with a bottom corner frequency of 0.01 Hz and four poles. This removes long period trends seen in the data (such as sustained water level response to the earthquake). In addition, the velocity waveforms and the fluid pressure were down-sampled to 1 sps. The obtained signals were used for cross-correlation procedure.

6 RESULTS

6.1 Tides

The 2 yr measured water pressure time series and calculated tides were divided to three months segments. Cross-correlation between measured water pressure fluctuations and calculated volumetric strain due to tide was calculated for each segment. The amplitude response and phase shift between the two time series are identical for each segment and do not vary in time. This implies that the elastic and hydrological aquifer properties are stable and are not affected by physical processes. Time series analysis using BAYTAP-G (Tamura *et al.* 1991) of the 3 yr record gives the phase shift, $\theta = 170$ deg and amplitude, $\frac{p_f}{W} = 3.7$ GPa m^2 s^{-2}. Using eq. (5), the term $BK_u\frac{1-2\nu_u}{1-\nu_u}$ was calculated to be 5.22 GPa. The actual coefficient BK_u of eq. (2), that relates pore pressure to volumetric strain could be calculated now only for a given Poisson's ratio. Transmissivity calculated using Hsieh *et al.* (1987) model gives $T = 4$E-5 m^2 s^{-1} (see Appendix B).

6.2 The Love and Rayleigh phases

We defined a time-window containing the Love and Rayleigh waveforms, and then applied cross-correlation searching for a best-fit solution for different equations, within a ±100 s overlap. The attempt to find a correlation between measured water pressure and water pressure calculated from radial strain results with $BK_u\frac{1-2\nu_u}{1-\nu_u} = 2.95$ GPa, low correlation $R^2 = 0.53$ and very low correlation for Love wave (Fig. 4a). Similarly, the correlation between measured water pressure and water pressure calculated from deviatoric strain results with $N = 6.9$ GPa, low correlation $R^2 = 0.53$ (Fig. 4b). The best correlation is achieved when including the effect of both radial and deviatoric strains for all surface wave phases (eq. 11). The solution found exhibits very high correlation (Fig. 5b), resulting in $BK_u\frac{1-2\nu_u}{1-\nu_u} = 3.87$ GPa, $N = 8.5$ GPa and $R^2 = 0.89$ (Fig. 6).

6.3 The *P* and *S* phases

Because the strain components in *P* and *S* waveforms are not well resolved, instead of searching for the best fit BK_u and N values (eq. 2), we used the results obtained by the Love and Rayleigh cross-correlation procedure. The BK_u value was calculated assuming Poisson's ratio to be within the range $\nu_u = 0.3-0.4$. As expected, the correlation is lower than the Love and Rayleigh, but still quite high, with R^2 above 0.67 (Fig. 5a).
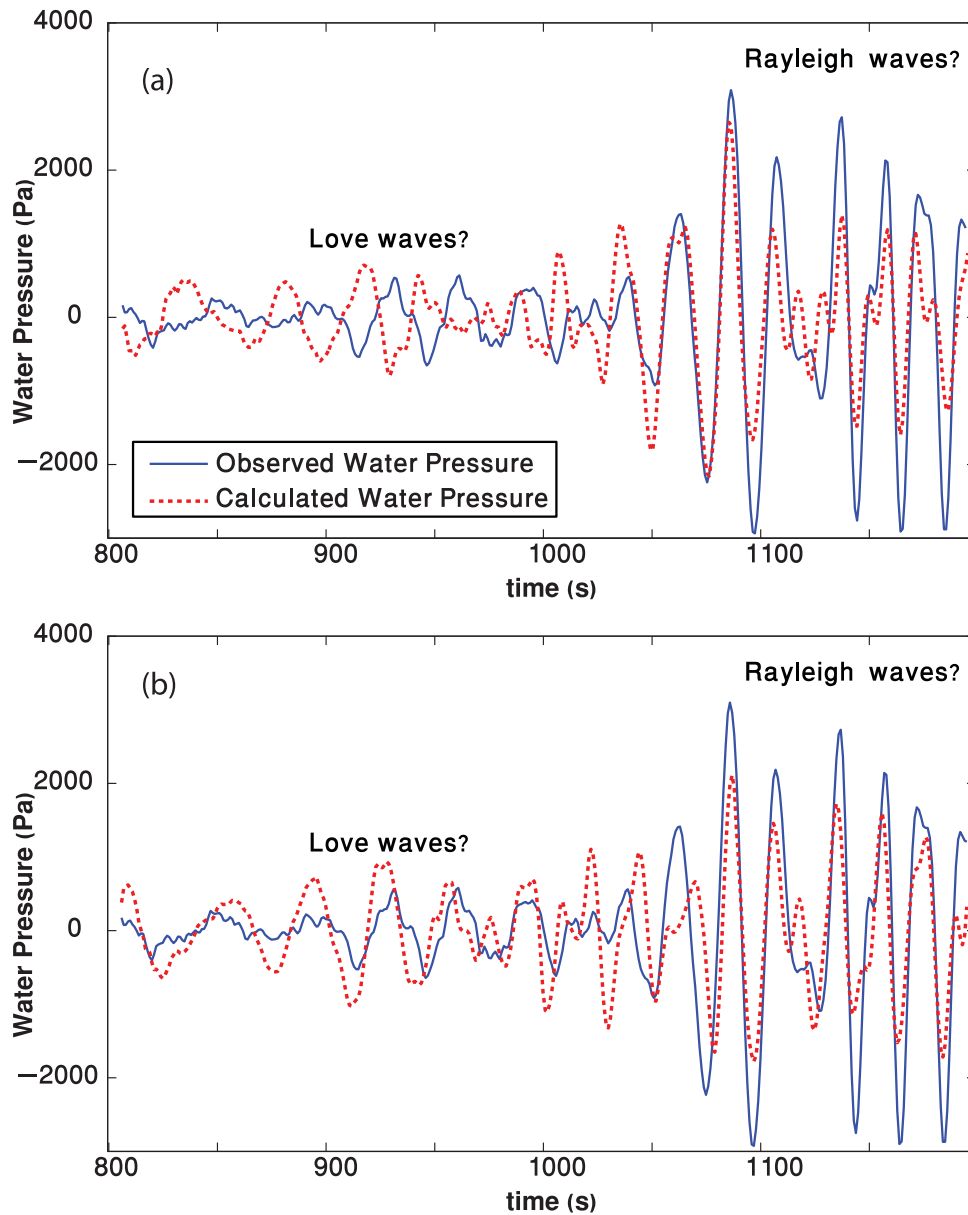
Figure 4. Observed and calculated well water pressure in Gomè 1 well in response to the distant ($\Delta = 26.469°$) Pakistan earthquake, assuming (a) only volumetric strain coupling and (b) only deviatoric strain coupling.

7 DISCUSSION

We suggest here that the calculated properties from the correlation between tides or seismic waves and water pressure represent the actual elastic properties of the aquifer with negligible coupling effect of the well and the aquifer. We estimated the amplification effect using Kitagawa *et al.* (2011) calculation for a volume of Gomè 1 well (18 m^3) and the transmissivity calculated from pumping tests at Gomè 1 well ($T = 4 \times 10^{-4}$ m^2 s^{-1}). Therefore, the calculated elastic properties represent the actual values of the aquifer. Both tidal and seismic analysis resulted with similar quantities of $BK_u \frac{1-2\nu_u}{1-\nu_u}$ equal to 5.2 GPa by tidal analysis, and 3.9 GPa by the seismic study. $N = 8.5$ GPa was obtained by the seismic study. This surprisingly high value suggests that water level oscillates not only due to the volumetric strain variations, but also due to deviatoric strain changes.

The 'dilatancy' behaviour was suggested to form by the existence of cracks in the rock (Brace *et al.* 1966). Lockner & Stanchits (2002) experimentally showed that the sensitivity of pore pressure change to the deviatoric stress increases with increasing stress level. Therefore, water level response to deviatoric stress variations depends on the density of the existing cracks and the level of the background tectonic stress. A rock with no cracks will show no dependency with deviatoric stress ($N = 0$) and damaged rock will show high water level response. Enhanced water level response to deviatoric stress variation ($N > 0$) is expected for heavily damaged rocks in active tectonic regions with high background stresses. Here we estimate the level of rock damage, α_D, which is needed to provide the observed response of the water pressure to the deviatoric strains. We define reasonable elastic properties of a damage-free material ($\alpha_D = 0$): drained and undrained Poisson's ratio to be $\nu = 0.15$, $\nu_u = 0.25$, and Skempton coefficient $B = 0.5$. These non-dimensional
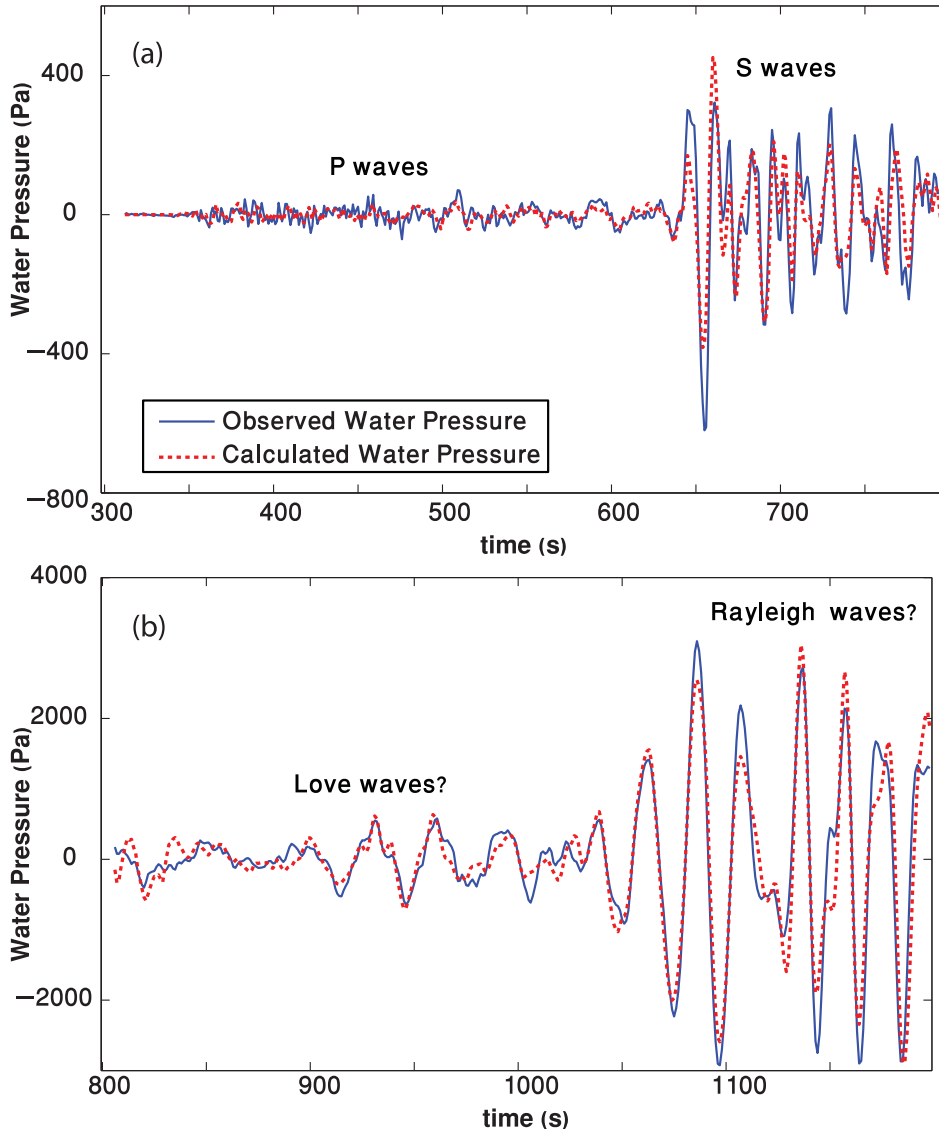
Figure 5. Observed and calculated well water pressure in Gomè 1 well in response to the distant ($\Delta = 26.469°$) Pakistan earthquake, for (a) body waves and (b) Surface waves.
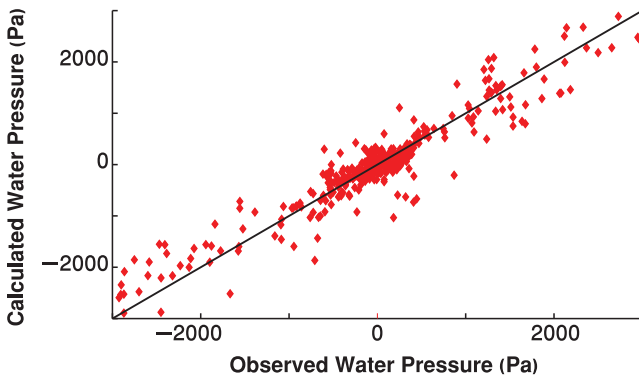

Figure 6. Cross-correlation between observed and calculated well water pressure in Gomè 1 well.

elastic properties change with damage and allow the calculation of the damage-dependent ratio between all elastic moduli. The dimensional results are then achieved by scaling the non-dimensional results using $BK_\mathrm{u}\frac{1-2\nu_\mathrm{u}(\alpha_D)}{1-\nu_\mathrm{u}(\alpha_D)} = 5.2$ GPa (tides) and 3.9 GPa (seis-

mic). The damage-dependent N-value is calculated using eq. (3) and shown in Fig. 7. The slightly different N-values calculated for tide and seismic analysis is shown in the grey shading. The value $N = 8.5$ GPa obtained by the seismic study corresponds to the range of the damage values from $\alpha_\mathrm{D} = 0.84$ (upper edge of the shaded area) to $\alpha_\mathrm{D} = 0.90$ (lower edge of the shaded area). High damage values mean that the rocks around the location of the Gomè 1 well are close to failure, which is compatible with geological and tectonic settings of the study area. The parameter A, calculated using eq. (4) for this damage state is between -0.25 and -0.5, corresponding to higher response of the fluid pressure to deviatoric stress change than suggested in previous studies. Wang (1997) suggested relatively low coupling with a value of $A = 0.2$ for the co-seismic water level changes near Parkfield. This value is only slightly below $A = 1/3$ of the linear poroelasicity without any dilatency. According to our estimation, the $A = 0.2$ value corresponds to $\alpha_\mathrm{D} \sim 0.45$. Stronger coupling was reported by Lockner & Stanchits (2002) based on the laboratory measurements with Berea sandstone samples deformed under different deviatoric stresses. They found that the value of the parameter A, decreases from ~ 0.25 at low deviatoric
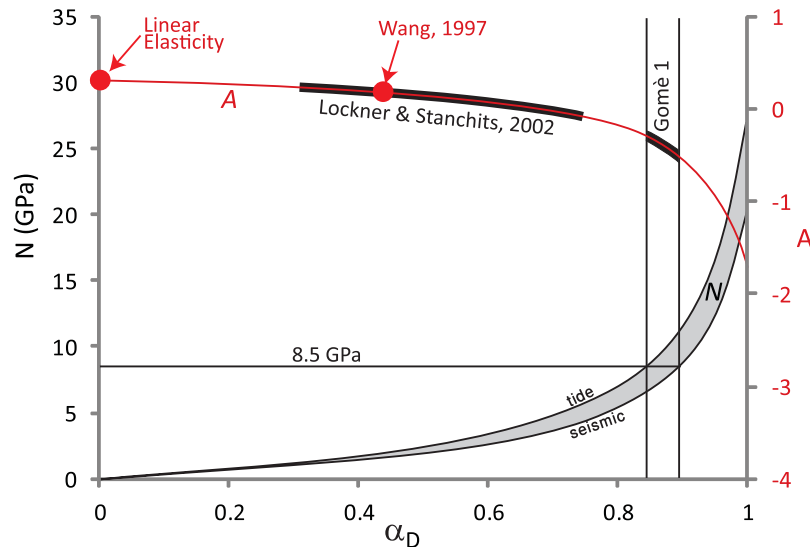
Figure 7. The deviatoric coupling terms: A and N, as a function of damage (α_D) for the tidal and seismic analysis. The seismic analysis result of $N = 8.5$ GPa corresponds to $-0.5 < A < -0.25$ and suggests $0.84 < \alpha_D < 0.9$. Results of Wang ([1997](#)) and Lockner & Stanchits ([2002](#)) were obtained in lower damage state.

stress to ~ -0.1 at higher deviatoric stress. We speculate here that pre-existing cracks were opened and probably new cracks were created in their laboratory samples during the differential loading up to 55 MPa under 17 MPa effective pressure. Their reported range of the A-values corresponds to $\alpha_D = 0.3$–0.75 shown in Fig. 7. The rock damage around the location of the Gomè 1 well estimated above also allows calculating the BK_u value. For $\alpha_D = 0.84$–0.9 the range of the undrained Poisson's ratio is $\nu_u = 0.38$–0.4 which gives $BK_u = 11$ GPa (seismic) and 14 GPa (tides). The relatively similar results of the seismic and tidal analysis shows the robustness of this procedure even compared to the direct laboratory experiments. For example, Hart & Wang ([1995](#)) measured the poroelastic properties of Berea sandstone and found that under mean effective stress of 10 MPa, the value of BK_u varies from 8.5 to 15.5 GPa between different samples. This variability of (~ 60 per cent) is much larger than the difference between the tidal and seismic analysis (25 per cent). In our study the water pressure is monitored at depth of ~ 400 m at Gomè 1 well, which corresponds to the similar ~ 10 MPa mean effective stress. Considering variations in the BK_u values measured in the laboratory by Hart & Wang ([1995](#)), we conclude that our calculations demonstrate a surprisingly good agreement between the tide and seismic analysis and both are well within the laboratory measured range for sandstones.

The data presented in this study are recorded from Gomè 1 well located within the damage zone of a major fault of the DST. The obtained hydroseismograms exhibit high water level oscillations in response to S and Love waves. If the rock is close to failure, the strain change caused by the travelling wave might increase the damage of the rock and change its poroelastic parameters. A slight change in the parameters might change the undrained response of the entire aquifer and change the water levels. We speculate that the sustained water level change observed in this study (Fig. 3d) may be a result of the small damage state variation of the aquifer.

8 CONCLUSIONS

Water levels from a closed well show strong oscillations caused by travelling seismic waves. These include strong water oscillations with the S and Love waves. We show that for the case of the Pakistan

earthquake, water oscillations induced by deviatoric strain in Gomè 1 are almost as high as oscillation induced by volumetric strain. The volumetric elastic properties calculated from tidal and seismic response of groundwater pressure are similar to other published sandstone data (Hart & Wang [1995](#)). However, the coupling between volumetric and deviatoric deformation calculated in this study are higher than the results of Wang ([1997](#)) and Lockner & Stanchits ([2002](#)). We find high value of $N = 8.5$ GPa that corresponds to $-0.5 < A < -0.25$ and suggests very high damage at Gomè 1 well. We propose that dilatancy, shown to occur in Gomè 1, is high in damaged rock (Sterling & Smets [1971](#); Brodsky *et al.* [2003](#)) and negligible in other wells where no Love-wave oscillations are observed in water level (Kano & Yanagidani [2006](#)). The significant coupling between shear and pore pressure should affect a wide variety of calculations, including standard Coulomb stress maps after every earthquake.

REFERENCES

Agnon, A. & Lyakhovsky, V., 1995. *Damage Distribution and Localization during Dyke Intrusion,* Balkema.

Biot, M.A., 1941. General Theory of Three-Dimensional Consolidation, *J. Appl. Phys.,* **12,** 155–164.

Brace, W.F., Paulding, B.W. & Scholz, C., 1966. Dilatancy in the fracture of crystalline rocks, *J. geophys. Res.,* **71,** 3939–3953.

Bredehoeft, J.D., 1967. Response of well-aquifer systems to Earth tides, *J. geophys. Res.,* **72,** 3075–3087.

Brodsky, E.E., Roeloffs, E., Woodcock, D., Gall, I. & Manga, M., 2003. A mechanism for sustained groundwater pressure changes induced by distant earthquakes, *J. geophys. Res.,* **108,** 2390, doi:10.1029/2002JB002321.

Byerlee, J., 1978. Friction of rocks, *Pageoph,* **116,** 615–626.

Cooper, H.H., Bredehoeft, J.D., Papadopulos, I.S. & Bennett, R.R., 1965. The response of well-aquifer systems to seismic waves, *J. geophys. Res.,* **70,** 3915–3926.

Doan, M.-L., Brodsky, E.E., Prioul, R. & Signer, C., 2006. *Tidal Analysis of Borehole Pressure: A Tutorial,* University of California.

Hamiel, Y., Liu, Y., Lyakhovsky, V., Ben-Zion, Y. & Lockner, D., 2004a. A viscoelastic damage model with applications to stable and unstable fracturing, *Geophys. J. Int.,* **159,** 1155–1165.

Hamiel, Y., Lyakhovsky, V. & Agnon, A., 2004b. Coupled evolution of damage and porosity in poroelastic media: theory and applications to deformation of porous rocks, *Geophys. J. Int.,* **156,** 701–713.

Hamiel, Y., Lyakhovsky, V. & Agnon, A., 2005. Rock dilation, nonlinear deformation, and pore pressure change under shear, *Earth planet. Sci. Lett.,* **237,** 577–589.

Hart, D.J. & Wang, H.F., 1995. Laboratory measurements of a complete set of poroelastic moduli for Berea sandstone and Indiana limestone, *J. geophys. Res.,* **100,** 17741–17751.

Henkel, D.J. & Wade, N.H., 1966. Plane strain tests on a saturated remoulded clay, *J. Soil Mech. & Found. Div.,* **92,** 67–80.

Holtz, R.D. & Kovacs, W.D., 1981. *An Introduction to Geotechnical Engineering,* Prentice-Hall.

Hsieh, P.A., Bredehoeft, J.D. & Farr, J.M., 1987. Determination of aquifer transmissivity from Earth tide analysis, *Water Resour. Res.,* **23,** 1824–1832.

Kano, Y. & Yanagidani, T., 2006. Broadband hydroseismograms observed by closed borehole wells in the Kamioka mine, central Japan: Response of pore pressure to seismic waves from 0.05 to 2 Hz, *J. geophys. Res.,* **111,** B03410, doi:10.1029/2005JB003656.

Keilis-Borok, V.I., 1989. *Seismic Surface Waves in a Laterally Inhomogeneous Earth,* Springer.

Kitagawa, Y., Itaba, S., Matsumoto, N. & Koizumi, N., 2011. Frequency characteristics of the response of water pressure in a closed well to volumetric strain in the high-frequency domain, *J. geophys. Res.,* **116,** B08301, doi:10.1029/2010JB007794.

Lay, T. & Wallace, T.C., 1995. *Modern Global Seismology,* Academic Press.

Levshin, A., Ratnikova, L. & Berger, J., 1992. Peculiarities of surface-wave propagation across central Eurasia, *Bull. seism. Soc. Am.,* **82,** 2464–2493.

Liu, L.-B., Roeloffs, E. & Zheng, X.-Y., 1989. Seismically induced water level fluctuations in the Wali Well, Beijing, China, *J. geophys. Res.,* **94,** 9453–9462.

Lockner, D.A. & Stanchits, S.A., 2002. Undrained poroelastic response of sandstones to deviatoric stress change, *J. geophys. Res.,* **107,** 2353, doi:10.1029/2001JB001460.

Lyakhovsky, V., Ben-Zion, Y. & Agnon, A., 1997. Distributed damage, faulting, and friction, *J. geophys. Res.,* **102,** 27635–27649.

Ohno, M., Wakita, H. & Kanjo, K., 1997. A water well sensitive to seismic waves, *Geophys. Res. Lett.,* **24,** 691–694.

Patton, H., 1980. Crust and upper mantle structure of the Eurasian continent from the phase velocity and Q of surface waves, *Rev. Geophys.,* **18,** 605–625.

Roeloffs, E., 1996. Poroelastic techniques in the study of earthquake-related hydrologic phenomena, in *Advances in Geophysics*, pp. 135–195, eds Renata, D. & Barry, S., Elsevier.

Roeloffs, E.A., 1998. Persistent water level changes in a well near Parkfield, California, due to local and distant earthquakes, *J. geophys. Res.,* **103,** 869–889.

Shearer, P.M., 2009. *Introduction to Seismology*, 2nd edn, Cambridge University Press.

Shi, Z., Wang, G., Manga, M. & Wang, C.Y., 2015. Continental-scale water-level response to a large earthquake, *Geofluids,* **15,** 310–320.

Skempton, A.W., 1954. The Pore-Pressure Coefficients A and B, *Géotechnique,* **4,** 143–147.

Sneh, A. & Weinberger, R., 2003. Geology of the Metulla quadrangle, northern Israel: implications for the offset along the Dead Sea rift, *Israel J. Earth Sci.,* **52,** 123–138.

Sterling, A. & Smets, E., 1971. Study of earth tides, earthquakes and terrestrial spectroscopy by analysis of the level fluctuations in a borehole at Heibaart (Belgium), *Geophys. J. Int.,* **23,** 225–242.

Tamura, Y., Sato, T., Ooe, M. & Ishiguro, M., 1991. A procedure for tidal analysis with a Bayesian information criterion, *Geophys. J. Int.,* **104,** 507–516.

Wang, C.-Y., Chia, Y., Wang, P.-L. & Dreger, D., 2009. Role of S waves and Love waves in coseismic permeability enhancement, *Geophys. Res. Lett.,* **36,** L09404, doi:10.1029/2009GL037330.

Wang, H.F., 1997. Effects of deviatoric stress on undrained pore pressure response to fault slip, *J. geophys. Res.,* **102,** 17943–17950.

Wang, H.F., 2000. *Theory of Linear Poroelasticity with Applications to Geomechanics and Hydrogeology,* Princeton University Press.

Yan, R., Woith, H. & Wang, R., 2014. Groundwater level changes induced by the 2011 Tohoku earthquake in China mainland, *Geophys. J. Int.,* **199,** 533–548.

APPENDIX A: FORMULATION OF POROELASTIC RESPONSE TO TRI-AXIAL LOADING

The expression for free energy, F, of a damaged poroelastic medium accounts for the nonlinear elastic properties that depend on the damage parameter, α_D (e.g. Lyakhovsky *et al.* 1997). Including both, the coupling between volumetric and shear deformations and the term for saturated material (Biot 1941), (Hamiel *et al.* 2004b) suggested the following energy equation:

$$F\left(\varepsilon_{ij}, \alpha_D\right) = \left(\frac{\lambda\left(\alpha_D\right)}{2} I_1^2 + \mu\left(\alpha_D\right) I_2 - \gamma\left(\alpha_D\right) I_1\sqrt{I_2}\right) + \frac{1}{2} M \cdot \left[\alpha_B I_1 - (\zeta - \phi)\right]^2, \tag{A1}$$

where λ and μ are Lamé constants, $I_1 = \varepsilon_{ij}\delta_{ij}$ and $I_2 = \varepsilon_{ij}\varepsilon_{ij}$ are the first and second invariants of the strain tensor ε_{ij} and γ is an additional modulus of a damaged solid which accounts for the material nonlinearity through the coupling term between volumetric and shear deformation. M and α_B are the Biot's modulus and coefficient for porous media, ζ is volume fluid content (ζ = Const for undrained conditions) and ϕ is material porosity. The product of the Biot's modulus and coefficient is equal to the product of the Skempton's volumetric coefficient B and the undrained bulk modulus K_u ($\alpha_B M = B K_u$).

Taking the derivative of the energy form eq. (A1) with respect to the strain and to the fluid content leads to the stress–strain and fluid pressure relations:

$$\sigma_{ij} = \frac{\partial F}{\partial \varepsilon_{ij}} = (\lambda\left(\alpha_D\right) - \gamma\left(\alpha_D\right)/\xi) I_1\delta_{ij} + (2\mu\left(\alpha_D\right) - \gamma\left(\alpha_D\right)\xi) \varepsilon_{ij} + B K_u \left[\alpha_B I_1 - (\zeta - \phi)\right]\delta_{ij} \tag{A2}$$

$$p = \frac{\partial F}{\partial \zeta} = B K_u \left[-I_1 + (\zeta - \phi)/\alpha_B\right]. \tag{A3}$$

The effective elastic moduli in eq. (A2) are functions of the strain invariants ratio, $\xi = I_1/\sqrt{I_2}$, which characterizes various states of loading. Its value varies between $\xi = -\sqrt{3}$ for 3-D compaction to $\xi = +\sqrt{3}$ for 3-D expansion; $\xi = \pm 1$ correspond to tension and compression, while $\varepsilon = 0$ corresponds to zero volumetric strain. The specific relation between the energy (eq. A1) and the damage state variable is established by making the elastic moduli functions of α_D. Given the available experimental constraints, (Agnon & Lyakhovsky 1995) assumed that the moduli μ and γ are linear functions of α_D and λ is constant:

$$\lambda = \lambda_0$$

$$\mu = \mu_{0+}\alpha_D\xi_0\ \gamma$$

$$\gamma = \alpha_D\gamma_r \tag{A4}$$

where λ_0, μ_0 and $\gamma = 0$ are the elastic moduli of a damage-free material ($\alpha_D = 0$), and $\lambda = \lambda_0$, $\mu = \mu_0 + \xi_0 \gamma_r$ and $\gamma = \gamma_r$ give the moduli values at maximum damage level ($\alpha_D = 1$). The parameter ξ_0 is a critical value of the strain invariants ratio at the onset of damage accumulation and is connected to the internal friction angle of the (Byerlee 1978) friction law for rocks (Agnon & Lyakhovsky 1995). During damage accumulation the modulus γ increases and the shear modulus μ decreases. This leads to material evolution from linear elastic solid ($\alpha_D = 0$) to strongly nonlinear behaviour and macroscopic brittle instability at a critical damage level ($\alpha_c = 1$ for $\xi = \xi_0$).

For the general case discussed in this study we assumed the elastic properties of the damage-free material ($\alpha_D = 0$) defining the Poisson ratio under drained conditions to be $\nu = 0.15$ and under undrained conditions $\nu_u = 0.25$. Taking $\xi_0 = -1$, typical value for sandstones (Hamiel *et al.* 2004a), the ratio between elastic moduli are: $\mu_0/\lambda_0 = 2.33$, $\gamma_r/\lambda_0 = 2.45$. Adopting $B = 0.5$ for the Skempton coefficient leads to $M/\lambda_0 = 2.84$ and $\alpha_B = 0.69$.

Hamiel *et al.* (2005) demonstrated that expressions for the stress tensor and fluid pressure (eqs A2 and A3) derived using energy potential (eq. A1) enable proper description of the rock dilation and related variation in fluid pressure as a function of shear stress that is widely observed in rock mechanics experiments. After lengthy derivations they provided an explicit relation for $A' = \partial p / \partial \tau_{oct}$ connecting fluid pressure change induced by variations in the octahedral stress under constant mean stress and undrained conditions (Hamiel *et al.* 2005):

$$A' = \frac{\sqrt{3} B K_u}{2 \left(\mu - \frac{1}{2} \gamma \xi \right) \sqrt{\frac{1}{\xi^2} - \frac{1}{3}} + \frac{\left(6\mu - \gamma \xi^3 \right) \left[K_u - \gamma \left(\frac{1}{\xi} + \frac{\xi}{3} \right) \right]}{3 \gamma \xi^3 \left(\frac{1}{\xi^2} - \frac{1}{3} \right)^{\frac{3}{2}}}}. \tag{A5}$$

Following Henkel & Wade (1966), the Skempton coefficient A is

$$A = \frac{1}{3} + \frac{\sqrt{2} A'}{3 B}. \tag{A6}$$

Gomè 1 well is located in a tectonically active area where stress state is close to the failure conditions ($\xi \approx \xi_0 = -1$). Substituting eq. (A5) into eq. (A6) and using $\xi = -1$ yields

$$A = \frac{1}{3} - \frac{4 K_u \gamma}{4 (2\mu + \gamma) \gamma - 3 (6\mu + \gamma)(K_u + 4/3\gamma)}. \tag{A7}$$

The parameter A depends on damage (α_D) through the elastic properties: μ, γ (eq. A4). Using $N = -4\mu B (A - \frac{1}{3})$, yields

$$N = \frac{8 B K_u \gamma (2\mu + \gamma)}{4 (2\mu + \gamma) \gamma - 3 (6\mu + \gamma)(K_u + 4/3\gamma)}. \tag{A8}$$

APPENDIX B: RESPONSE OF WATER PRESSURE IN GOMÈ 1 WELL TO SEISMIC WAVES AND EARTH TIDES

Kitagawa *et al.* (2011) developed an expression describing the hydraulic coupling between the aquifer and the well. They provided analytical solution for the response of the water level, X_0, in the well to observed volumetric strain, ε_0^{obs} (eq. 17 in Kitagawa *et al.* 2011):

$$\frac{X_0}{\varepsilon_0^{obs}} = -\frac{1}{A_{vs}} \frac{K_w A_w}{\rho g} \frac{\frac{K_u B}{\rho g A_w} \frac{2\pi T}{\omega V_w} - A_2 + i A_1}{\frac{K_w}{\rho g} \frac{2\pi T}{\omega V_w} - A_2 + i A_1}, \tag{B1}$$

where $A_{vs} = \frac{\varepsilon_0^{obs}}{\varepsilon_0}$ is the amplification factor of the volumetric strain observed in the well relative to the real volumetric strain (ε_0). In this study, ε_0 is calculated from the seismograms. K_w is the water bulk modulus; A_w is the amplification factor of well volume change due to elastic deformation; ρ is water density; K_u is the undrained bulk modulus; B is the Skempton coefficient; T is the transmissivity; ω is the frequency; V_w is the water volume within the borehole. The coefficients A_1 and A_2 are defined as

$$A_1 = \Phi \mathrm{Ker}(\alpha_s) - \Psi \mathrm{Kei}(\alpha_s) \tag{B2}$$

$$A_2 = \Psi \mathrm{Ker}(\alpha_s) + \Phi \mathrm{Kei}(\alpha_s) \tag{B3}$$

$$\Phi = \frac{-[\mathrm{Ker}_1(\alpha_s) + \mathrm{Kei}_1(\alpha_s)]}{\sqrt{2}\alpha_s \left[\mathrm{Ker}_1^2(\alpha_s) + \mathrm{Kei}_1^2(\alpha_s) \right]} \tag{B4}$$

$$\Psi = \frac{-[\mathrm{Ker}_1(\alpha_s) - \mathrm{Kei}_1(\alpha_s)]}{\sqrt{2}\alpha_s \left[\mathrm{Ker}_1^2(\alpha_s) + \mathrm{Kei}_1^2(\alpha_s) \right]} \tag{B5}$$

$$\alpha_s = \sqrt{\frac{\omega S}{T}} r, \tag{B6}$$

where S is the storativity and r is the radius of the borehole, $\mathrm{Ker}(\alpha_s)$, $\mathrm{Kei}(\alpha_s)$, $\mathrm{Ker}_1(\alpha_s)$ and $\mathrm{Kei}_1(\alpha_s)$ are Kelvin functions of order 0 and 1.

Eq. (B1) can be rewritten in terms of the ratio between the observed pressure, P_{obs}, and the water pressure due to the elastic deformation (eq. 4 in Kitagawa *et al.* 2011), $P_0 = -K_w A_w \varepsilon_0$:

$$\frac{P_{obs}}{P_0} = \frac{\frac{K_u B}{\rho g A_w} \frac{2\pi T}{\omega V_w} - A_2 + i A_1}{\frac{K_w}{\rho g} \frac{2\pi T}{\omega V_w} - A_2 + i A_1}. \tag{B7}$$

The amplitude of the eq. (B7) is

$$\left| \frac{P_{obs}}{P_0} \right| = \sqrt{\frac{\left(\frac{K_u B}{\rho g A_w} \frac{2\pi T}{\omega V_w} - A_2 \right)^2 + A_1^2}{\left(\frac{K_w}{\rho g} \frac{2\pi T}{\omega V_w} - A_2 \right)^2 + A_1^2}}. \tag{B8}$$

The tangent of the phase shift, θ, of eq. (B7) is

$$\tan \theta = \frac{\left(\frac{K_w}{\rho g} - \frac{K_u B}{\rho g A_w} \right) \frac{2\pi T}{\omega V_w} A_1}{\left(\frac{K_u B}{\rho g A_w} \frac{2\pi T}{\omega V_w} - A_2 \right) \left(\frac{K_w}{\rho g} \frac{2\pi T}{\omega V_w} - A_2 \right) + A_1^2}. \tag{B9}$$

For Earth tides, Hsieh *et al.* (1987) showed that

$$\left| \frac{P_{obs}}{P_0} \right| = \sqrt{E^2 + F^2} \tag{B10}$$

$$\tan \theta = -\frac{F}{E}, \tag{B11}$$

where

$$E \approx 1 - \frac{\omega r^2}{2T} \mathrm{Kei}(\alpha_s) \tag{B12}$$

$$F \approx \frac{\omega r^2}{2T} \mathrm{Ker}(\alpha_s). \tag{B13}$$

The parameters of Gomè 1 well are listed in Table B1. T is determined from tidal analysis. S is determined from the following

Table B1. Parameters of Gomè 1 well.

Parameter	Value
T	4.E-5 m^2 s^{-1}
S	1.E-4
r	0.1143 m
ω	Seismic—0.21 1 s^{-1}; tides—1.45E-4 1 s^{-1}
V_w	16.42 m^3
$K_u B$	10 GPa
K_w	2.2 GPa
A_w	3–6

equations (Wang 2000):

$$S_\varepsilon = \frac{\alpha_B}{K_u B} \tag{B14}$$

$$S = S_s b \approx \frac{S_\varepsilon}{\rho g} b, \tag{B15}$$

where $\alpha_B = 1$ is Biot coefficient, S_s is the specific storage and $b = 100$ m is the thickness of the aquifer. The value of A_w is controlled by the circular shape of the borehole, the iron casing, the grout and the surrounding rocks. As mentioned by Kitagawa *et al.* (2011), there is no method to independently estimate A_w. Following their estimation, we use $A_w = 3$–6.

For seismic response, the following variables are: $\alpha_s = 0.0083$, Ker(α_s)= 2.6, Kei(α_s)= -0.78, Ker$_1$(α_s)= 11.96, Kei$_1$(α_s)= -8.62, $\Phi = -0.131$, $\Psi = -0.81$, $A_1 = -0.97$ and $A_2 = -2.0$. The amplitude is then $|\frac{P_{obs}}{P_0}| = 0.78$–1.5. Therefore, the amplification due to aquifer properties and geometrical dimensions of the well are negligible.

For Earth tides response, the following variables are: $\alpha_s = 0.00218$, Ker(α_s)= 6.244, Kei(α_s)= -0.785, E = 1.02, F = -0.148, $\theta = 171$ deg, and $|\frac{P_{obs}}{P_0}| = 1.03$. The phase shift, $\theta = 170$ deg and $S = 1.$E-4, which are obtained by the tidal analysis agree with $T = 4.$E-5 m^2 s^{-1}.